P-Q Theory-based Dynamic Load Modelling in Short-Circuit Analysis

Karthik Rajashekaraiah
Giovanni De Carne
Institute for Technical Physics
Karlsruhe Institute of Technology
Karlsruhe, Germany
karthik.rajashekaraiah@kit.edu
giovanni.carne@kit.edu

Cosimo Iurlaro, Mauro Semeraro
Sergio Bruno
Dep. of Electr. and Inform. Engineering (DEI)
Politecnico di Bari
Bari, Italy
cosimo.iurlaro@poliba.it, m.semeraro12@studenti.poliba.it
sergio.bruno@poliba.it

***Abstract*—Short-circuit analysis is essential for determining the fault current rating of different protection devices installed in a power system network. Usually, the inaccuracy in short-circuit current calculation is due to the fact of neglecting the effect of load during short circuit analysis. This paper shows the symmetrical short-circuit analysis of a balanced grid considering the effect of loads using the instantaneous p-q theory based load models. Comparison of the results obtained by using the p-q theory-based load model with the MATLAB/Simulink three-phase dynamic load model establishes better computational performance in a real-time environment without losing much in accuracy.**

***Index Terms*—Load Modelling, dynamic load, Real-time computation, instantaneous p-q theory, p-q theory-based load (PQL), symmetrical fault**

I. Introduction

During normal operating conditions, electrical devices work with a certain rated current. However, these currents may exceed the normal values during faults, causing serious damage if the fault currents are not limited or interrupted. In distribution systems, the faults causes around 80% of service failures [1].

The short-circuit faults in power systems can be classified as symmetrical faults and unsymmetrical faults. The symmetrical faults are triple line-to-ground (LLLG) and triple line (LLL) faults. Whereas, the unsymmetrical faults are namely double line-to-ground (LLG), line-to-line (LL) and single line-to-ground (LG) faults. The unsymmetrical faults are the common faults, while the symmetrical ones are rare. However, from an electrical point of view, the symmetrical faults result in high currents and they can damage or destroy the connected devices. Hence, the protection systems should quickly work to protect the healthy part of the system during the occurrence of the symmetrical faults.

Fault analysis is a process of evaluating the system currents and voltages under different short-circuit conditions. The analysis of faults is essential to improve customer security and reliability. For many years, the symmetrical components based approach is used in power industry for short circuit analysis [2], [3]. In the calculation of bus voltage and post-fault branch currents, the effect of loads have been neglected [4]. In order to have reliable results in the short circuit analysis, accurate load model has to be modelled as it plays a critical role [5]–[7]. Improper load models causes inaccurate calculation of short-circuit currents and may lead to problems in settings of the relays.

Modelling a general load model is a challenge as it varies due to nature, external dependencies (such as frequency, voltage, temperature, etc.) and power level. Measurement based approach is used for modelling load model in majority of power system simulation software due to the lack of load characteristics information [8], [9], where the dynamics of the loads are interpreted using exponential dynamic model or induction motor model [10]. However, model detailed models [11] imply also a higher computational effort for the simulators, that can reduce the size of the analyzed grid or increase the simulation time [12]. Furthermore, the Power Hardware-in-the-Loop (PHIL) and digital real-time simulations [13] require dynamic load models to mimic the behaviour of complex grids [14] and emulate dynamic distributed active resources [15].

In this paper, a computationally lighter three-phase dynamic load model for real-time power system simulations has been implemented. The proposed load model is based on the instantaneous p-q theory [16] and aims to be a computationally lighter model alternative to the three-phase Dynamic Load model proposed by MATLAB/Simulink (SDL). The enhancements are incorporated in the p-q theory-based dynamic load (PQL) by eliminating the heavy computational burden blocks for simulating the model in real-time environment. The implemented PQL model has been incorporated on the existing large network benchmark (SimBench medium voltage (MV) urban network [17]). Study results show that the PQL model implemented has better accuracy with respect to SDL model and higher computational performance in a real-time environment.

This paper is organised as follows: Section II introduces to the concept of p-q theory. In section III, the test results obtained in real-time simulations are presented by applying triple line-to-ground (LLLG) fault to SimBench medium voltage urban network. Finally in section IV, the conclusions are drawn.

II. P-Q THEORY

This section describes the mathematical approach of p-q theory introduced by [16]. For the sake of simplicity, the concept of p-q theory is discussed for three-phase, three-wire balanced systems, even though it is also applicable to four-wire systems. The positive, negative, and zero sequences should be considered in the case of unbalanced systems. The time dependency of electrical variables such as voltage, current, etc. is omitted to make the mathematical formulation more readable. The p-q theory is defined as a set of time-domain power equations, based on instantaneous values. This theory considers the three-phase system as a unit, not a superposition or sum of three single-phase circuits, and it is valid for both steady-state and transient analysis.

The p-q theory works with voltage and current in the $\alpha\beta 0$ coordinates, which can be expressed as in (1). v_α and v_β are obtained from the amplitude of three-phase voltage waveforms v_a,v_b and v_c, by power-variant transformation as mentioned in (2).

$$\begin{aligned} v_{\alpha\beta} &= v_\alpha + \jmath v_\beta \\ i_{\alpha\beta} &= i_\alpha + \jmath i_\beta \end{aligned} \tag{1}$$

$$\begin{bmatrix} v_\alpha \\ v_\beta \end{bmatrix} = \frac{2}{3}\begin{bmatrix} 1 & -\frac{1}{2} & -\frac{1}{2} \\ 0 & \frac{\sqrt{3}}{2} & -\frac{\sqrt{3}}{2} \end{bmatrix}\begin{bmatrix} v_a \\ v_b \\ v_c \end{bmatrix} \tag{2}$$

Since the instantaneous complex power s can be expressed as the product of voltage vector v and the conjugate of current vector i^* (3), based on this expression, it is possible to calculate the instantaneous active and reactive powers as in (4). It is essential to underline that the complex power definition (3) is valid during both transients and steady states because instantaneous voltages and currents are considered.

$$\begin{aligned} s = v_{\alpha\beta} \cdot i^*_{\alpha\beta} &= (v_\alpha + \jmath v_\beta)(i_\alpha - \jmath i_\beta) \\ &= (v_\alpha i_\alpha + v_\beta i_\beta) + \jmath(v_\beta i_\alpha - v_\alpha i_\beta) \end{aligned} \tag{3}$$

$$\begin{aligned} p &= v_\alpha i_\alpha + v_\beta i_\beta \\ q &= v_\beta i_\alpha - v_\alpha i_\beta \end{aligned} \tag{4}$$

From the instantaneous active and reactive power expressions in (4), the instantaneous currents in α-β coordinates can be calculated as in (5).

$$\begin{bmatrix} i_\alpha \\ i_\beta \end{bmatrix} = \frac{1}{v_\alpha^2 + v_\beta^2}\begin{bmatrix} v_\alpha & v_\beta \\ v_\beta & -v_\alpha \end{bmatrix}\begin{bmatrix} p \\ q \end{bmatrix} \tag{5}$$

Exploding the right-hand side of the equation (5), as in (6), it is easier to obtain the expressions of the active and reactive components of the instantaneous currents in α-β coordinates (7-10).

$$\begin{aligned} \begin{bmatrix} i_\alpha \\ i_\beta \end{bmatrix} &= \frac{1}{v_\alpha^2 + v_\beta^2}\begin{bmatrix} v_\alpha & v_\beta \\ v_\beta & -v_\alpha \end{bmatrix}\begin{bmatrix} p \\ 0 \end{bmatrix} \\ &+ \frac{1}{v_\alpha^2 + v_\beta^2}\begin{bmatrix} v_\alpha & v_\beta \\ v_\beta & -v_\alpha \end{bmatrix}\begin{bmatrix} 0 \\ q \end{bmatrix} \\ &= \begin{bmatrix} i_{\alpha p} \\ i_{\beta p} \end{bmatrix} + \begin{bmatrix} i_{\alpha q} \\ i_{\beta q} \end{bmatrix} \end{aligned} \tag{6}$$

$$i_{\alpha p} = \frac{v_\alpha}{v_\alpha^2 + v_\beta^2} p \tag{7}$$

$$i_{\alpha q} = \frac{v_\beta}{v_\alpha^2 + v_\beta^2} q \tag{8}$$

$$i_{\beta p} = \frac{v_\beta}{v_\alpha^2 + v_\beta^2} p \tag{9}$$

$$i_{\beta q} = \frac{-v_\alpha}{v_\alpha^2 + v_\beta^2} q \tag{10}$$

The reference currents i_{abc} (11) can be obtained through the inverse Clarke-transformation from (5).

$$\begin{bmatrix} i_a \\ i_b \\ i_c \end{bmatrix} = \sqrt{\frac{2}{3}}\begin{bmatrix} 1 & 0 \\ -\frac{1}{2} & \frac{\sqrt{3}}{2} \\ -\frac{1}{2} & -\frac{\sqrt{3}}{2} \end{bmatrix}\begin{bmatrix} i_\alpha \\ i_\beta \end{bmatrix} \tag{11}$$

Based on the p-q theory described above, a three-phase load model was realised in the MATLAB/Simulink simulation environment. The three-phase p-q theory-based load model (PQL) has been designed to be computationally low but at the same time to have all the features included in the three-phase Dynamic Load (SDL) included in the Simulink library, i.e. capable of following external active and reactive power set-points but also behaving as an exponential load model. In Fig. 1, an exhaustive block diagram representation of the model was shown. This diagram has been designed in such a way that it is easy to reproduce the load model proposed in this paper.

At the point of interconnection of the load model to the grid, the phase voltages v_{abc} are measured, in per unit (p.u.), and transformed into v_α and v_β according to (2). The complex voltage value $v_{\alpha\beta}$ is calculated according to (1) and the magnitude of this signal is provided to a block where the exponential load model equations have been implemented. As inputs of this model, others to the voltage magnitude, the initial active and reactive powers (Po, Qo) and exponents controlling the nature of the exponential load model (n_p, n_q) have to be provided. The exponential load model behaviour is bypassed if the active and reactive power references (p, q) are provided externally.

The active and reactive power references (p, q) are compared to the active and reactive power calculated (p_c, q_c) according to (4) and the error is fed to a Proportional-Integral controller (PI) in order to follow the reference values. Moreover, to speed up the response of the system, a feed-forward technique is also considered in the model. The corrected active and reactive powers (p^*, q^*) are used to calculate the currents i_α and i_β according to (5). In order to reduce the discontinuities in the current signals and to have smooth transitions, the currents i_α and i_β are filtered using a first-order Butterworth filter with a cut-off frequency of $400Hz$.

By using (11), the filtered currents i_α and i_β are transformed into currents i_{abc}. These currents are used as references for controlled-current sources to represent the load behaviour. As can be noted, blocks that burden the calculation, such as PLL,

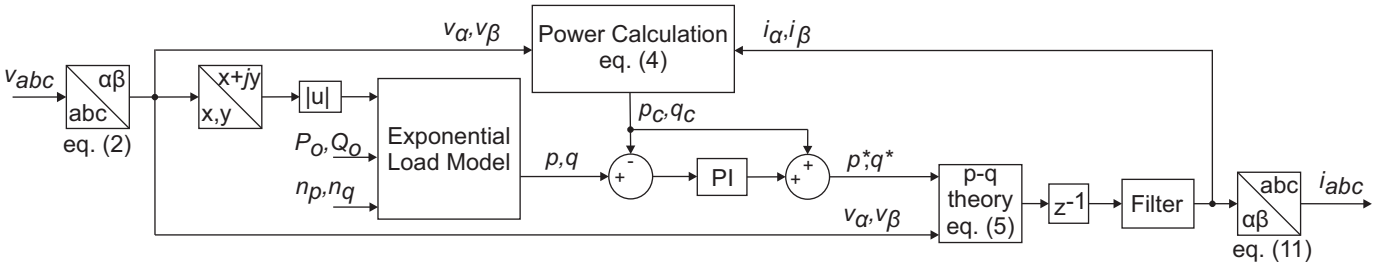

Fig. 1: Schematic of the three-phase p-q theory-based load (PQL)

mean and $abc - dq0$ transformation (and vice versa) are not present in the model.

III. Simulation Results

To validate the three-phase p-q theory-based dynamic load, the SimBench medium voltage urban network is considered by neglecting switches and open lines for the sake of simplicity. The SimBench is an open-source dataset containing different benchmark networks based on power grids in Germany [17]. The network data can be found in [18].

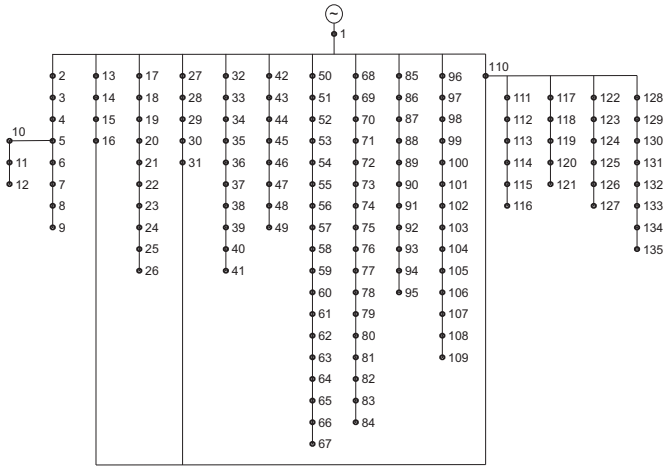

Fig. 2: SimBench MV urban metwork

The network, shown in Fig. 2, consists of 134 supply points (135 buses in total, no load is connected at node 110) which are divided into 14 feeders. The feeders are relatively short, with lengths ranging from 0.7 to 4.7 km. The sums of the loads and Distributed Energy Resources (DERs) are approximately 49.7 MW and 13.6 MW, respectively. The network, with a rated voltage of 10 kV, is fed by two in-line high voltage to medium voltage transformers (HV/MV) of 63 MVA, connected in parallel. However, for the sake of simplicity, the transformers have been neglected and the network has been assumed to be fed directly by an equivalent power source. The network was simulated using OPAL-RT's OP5700 simulator, with two CPU cores at a time step of 50μs.

The short-circuit test was performed to study the symmetrical fault analysis using p-q theory-based dynamic load. The loads were set as constant power load and a three-phase to ground fault (LLLG-fault) was applied at the node 135. The fault was applied for a time interval of $0.1s$, from $0.4s$ to $0.5s$, to observe the behaviour of voltages and currents at the point of load connection during fault occurrence. A similar test was conducted by replacing the PQL model with the SDL model in the network under test, and the comparison analysis was performed as shown in Fig. 3.

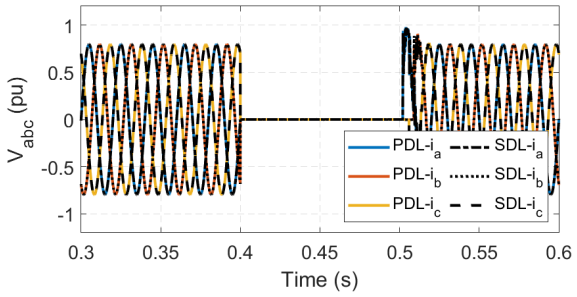

(a) v_{abc} at node-135

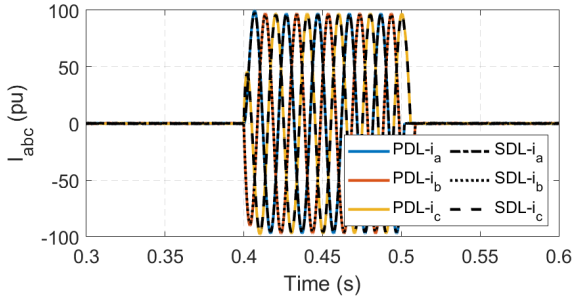

(b) i_{abc} at node-135

Fig. 3: Three-phase voltages and currents at node-135 due to LLLG fault

From the Fig. 3, we observe that the voltages and currents are oscillating normally at $50Hz$ before the fault occurs. We also see that the voltage is normal and near to operating voltage and current being very low. But, when the fault occurs at $0.4s$, the voltage drops to $0V$ for all the phases, while the currents become high, nearly $100pu$. When the fault is removed at $0.5s$, the voltages and currents come to normal state.

In Fig. 4a and Fig. 4b, the three-phase rms voltage and current waveforms are shown. We observe that the rms voltage and current have same response as the SDL model

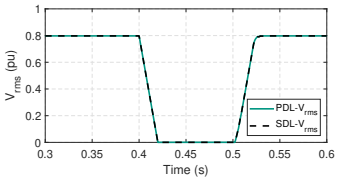

(a) Three-phase rms voltage at node-135

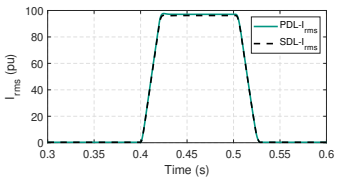

(b) Three-phase rms current at node-135

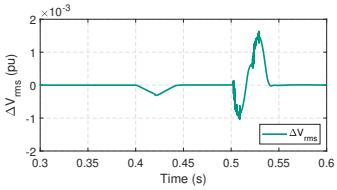

(c) Deviation of Three-phase rms voltage at node-135

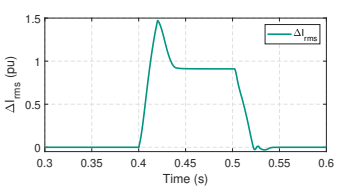

(d) Deviation of Three-phase rms current at node-135

Fig. 4: Three-phase rms voltage and current at node-135 due to LLLG fault

except at the occurrence and clearance of the fault. The maximum deviation of rms voltage and rms current with respect to SDL model was observed to be around 0.18% and 1.5% respectively, which is negligible. Fig. 4c and Fig. 4d shows the deviation in three-phase rms voltage and current with respect to SDL model respectively.

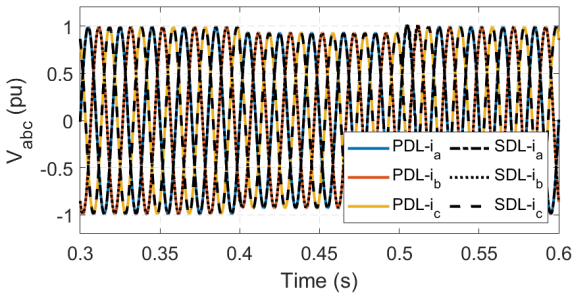

(a) v_{abc} at node-110

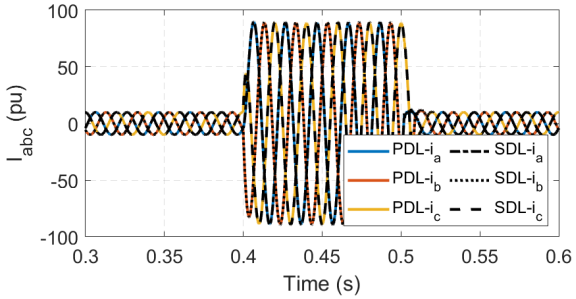

(b) i_{abc} at node-110

Fig. 5: Three-phase voltages and currents at node-110 due to LLLG fault

The measurements were also taken at node 110 in the network under study to analyse the impact of the fault caused at node 135. Fig. 5 shows the impact of the fault on voltages and currents at node 110. The voltages exert some voltage dip due to the occurrence of fault at node 135 but, not as much as we observe at the node 135. However, the currents experience a a more significant impact due to the occurrence of the fault. It is also observed that the voltages and currents of the PDL model fit with the results of the SDL model.

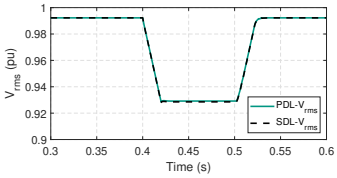

(a) Three-phase rms voltage at node-110

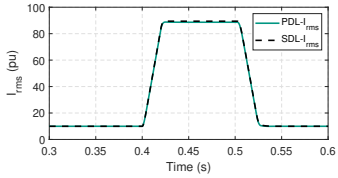

(b) Three-phase rms current at node-110

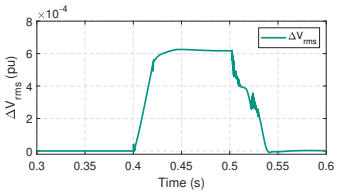

(c) Deviation of Three-phase rms voltage at node-110

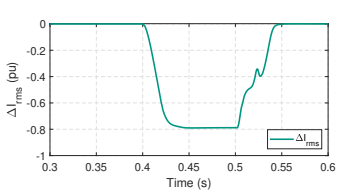

(d) Deviation of Three-phase rms current at node-110

Fig. 6: Three-phase rms voltage, currents and its deviation with respect to SDL model at node-110 due to LLLG fault

The three-phase rms voltage and current at node-110 is shown in Fig 6a and Fig. 6b respectively. The PDL model has the similar response as the SDL model during steady state and fault occurrence. The maximum deviation of the rms voltage is around 0.06% and rms current is 0.8% at node-110 with respect to SDL model, which can be considered negligible.

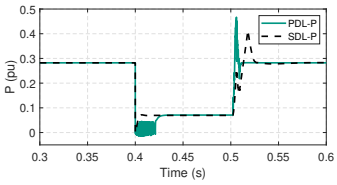

(a) Active Power

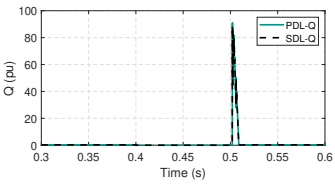

(b) Reactive Power

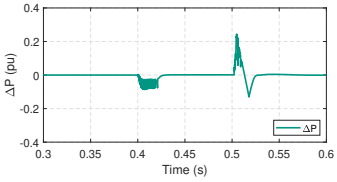

(c) Deviation in active power

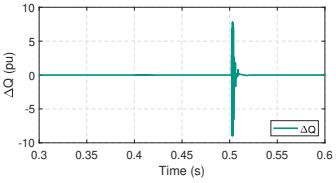

(d) Deviation in reactive power

Fig. 7: Active power, Reactive power and its deviation in Load-136 due to LLLG-fault

The active and reactive power of the load-136 connected at node-135 is shown in Fig.7a and Fig.7b respectively. The active and reactive power of the PDL and SDL model are observed to coincide with each other during steady-state and

fault occurrence duration. The deviation of active and reactive power is shown in Fig. 7c and Fig. 7d.

IV. Conclusion

The instantaneous p-q theory-based load model is presented for digital real-time simulation. The three-phase p-q load model is proposed as an alternative to the MATLAB/Simulink three-phase dynamic load with significant improvements. The improvements are made for real-time simulation by eliminating the computational burden blocks such as PLL, mean, and $dq0 - abc$ transformation. In this work, the three-phase p-q theory-based load model was used for perform symmetrical fault analysis over Simulink three-phase dynamic load model. The results show that the p-q theory-based load model has the responses as a three-phase Simulink dynamic load without losing much in accuracy.

V. Acknowledgment

This work has been supported by the Helmholtz Association under the program "Energy System Design" and under the Helmholtz Young Investigator Group "Hybrid Networks" (VH-NG-1613).

References

[1] C.-L. Su and J.-H. Teng, "Economic evaluation of a distribution automation project," *Industry Applications, IEEE Transactions on*, vol. 43, pp. 1417 – 1425, 12 2007.

[2] J. J. Grainger and W. D. Stevenson Jr, *Power system analysis*. McGraw-Hill series in electrical and computer engineering, 1994.

[3] M. Abdel-Akher and K. M. Nor, "Fault analysis of multiphase distribution systems using symmetrical components," *IEEE Transactions on Power Delivery*, vol. 25, no. 4, p. 2931 – 2939, 2010, cited by: 91. [Online]. Available: https://www.scopus.com/inward/record.uri?eid=2-s2.0-77956993012&doi=10.1109%2fTPWRD.2010.2046682&partnerID=40&md5=aede25b5300986a10e1d01f9082cbdd7

[4] A. Mathur, V. Pant, and B. Das, "Unsymmetrical short-circuit analysis for distribution system considering loads," *International Journal of Electrical Power & Energy Systems*, vol. 70, pp. 27–38, 2015.

[5] A. Tan, "Transformer and load modeling in short circuit analysis for distribution systems," *IEEE Transactions on Power Systems*, vol. 12, no. 3, p. 1315 – 1322, 1997, cited by: 39. [Online]. Available: https://www.scopus.com/inward/record.uri?eid=2-s2.0-0031197278&doi=10.1109%2f59.630476&partnerID=40&md5=381abdf15726833abfcbff9abc0009de

[6] M. Todorovski and D. Rajicic, "Handling three-winding transformers and loads in short circuit analysis by the admittance summation method," *IEEE Transactions on Power Systems*, vol. 18, no. 3, p. 993 – 1000, 2003, cited by: 11. [Online]. Available: https://www.scopus.com/inward/record.uri?eid=2-s2.0-0041524279&doi=10.1109%2fTPWRS.2003.814850&partnerID=40&md5=a6c9622f53bada353a554af5d5029a8d

[7] M.-S. Chen and W. E. Dillon, "Power system modeling," *Proceedings of the IEEE*, vol. 62, no. 7, pp. 901–915, 1974.

[8] J. V. Milanovic, K. Yamashita, S. M. Villanueva, S. Ž. Djokic, and L. M. Korunović, "International industry practice on power system load modeling," *IEEE Transactions on Power Systems*, vol. 28, no. 3, pp. 3038–3046, 2012.

[9] A. J. Collin, G. Tsagarakis, A. E. Kiprakis, and S. McLaughlin, "Development of low-voltage load models for the residential load sector," *IEEE Transactions on Power Systems*, vol. 29, no. 5, pp. 2180–2188, 2014.

[10] A. Arif, Z. Wang, J. Wang, B. Mather, H. Bashualdo, and D. Zhao, "Load modeling—a review," *IEEE Transactions on Smart Grid*, vol. 9, no. 6, pp. 5986–5999, 2018.

[11] G. De Carne, M. Langwasser, M. Ndreko, R. Bachmann, R. W. De Doncker, R. Dimitrovski, B. J. Mortimer, A. Neufeld, F. Rojas, and M. Liserre, "Which deepness class is suited for modeling power electronics?: A guide for choosing the right model for grid-integration studies," *IEEE Industrial Electronics Magazine*, vol. 13, no. 2, pp. 41–55, 2019.

[12] G. De Carne, G. Lauss, M. H. Syed, A. Monti, A. Benigni, S. Karrari, P. Kotsampopoulos, and M. O. Faruque, "On modeling depths of power electronic circuits for real-time simulation – a comparative analysis for power systems," *IEEE Open Access Journal of Power and Energy*, vol. 9, pp. 76–87, 2022.

[13] A. Benigni, T. Strasser, G. De Carne, M. Liserre, M. Cupelli, and A. Monti, "Real-time simulation-based testing of modern energy systems: A review and discussion," *IEEE Industrial Electronics Magazine*, vol. 14, no. 2, pp. 28–39, 2020.

[14] E. Bompard, S. Bruno, A. Cordoba-Pacheco, C. Diaz-Londono, G. Giannoccaro, M. La Scala, A. Mazza, and E. Pons, "Latency and simulation stability in a remote power hardware-in-the-loop cosimulation testbed," *IEEE Transactions on Industry Applications*, vol. 57, no. 4, pp. 3463–3473, 2021.

[15] S. Bruno, G. Giannoccaro, C. Iurlaro, M. La Scala, M. Menga, C. Rodio, and R. Sbrizzai, "Fast frequency support through led street lighting in small non-synchronous power systems," *IEEE Transactions on Industry Applications*, vol. 59, no. 2, pp. 2277–2287, 2022.

[16] H. Akagi, E. H. Watanabe, and M. Aredes, *Instantaneous power theory and applications to power conditioning*. John Wiley & Sons, 2017.

[17] S. Meinecke, S. Drauz, A. Klettke, D. Sarajlic, J. Sprey, C. Spalthoff, C. Kittl, M. Braun, A. Moser, and C. Rehtanz, "Simbench documentation—electric power system benchmark models," Technical Report EN-1.0. 0 University of Kassel, Fraunhofer IEE, RWTH Aachen ..., Tech. Rep., 2020.

[18] "https://simbench.de/en/download/datasets/," - *Simbench Medium voltage data (1-MV-semiurban–0-sw)*. [Online]. Available: https://simbench.de/en/download/datasets/